NANO · MICRO small
www.small-journal.com

Advancement of Ag–Graphene Based Nanocomposites: An Overview of Synthesis and Its Applications

Kai He, Zhuotong Zeng, Anwei Chen, Guangming Zeng, Rong Xiao,* Piao Xu, Zhenzhen Huang, Jiangbo Shi, Liang Hu, and Guiqiu Chen*

Graphene has been employed as an excellent support for metal nanomaterials because of its unique structural and physicochemical properties. Silver nanoparticles (AgNPs) with exceptional properties have received considerable attention in various fields; however, particle aggregation limits its application. Therefore, the combination of AgNPs and graphene based nanocomposites (Ag–graphene based nanocomposites) has been widely explored to improve their properties and applications. Excitingly, enhanced antimicrobial, catalytic, and surface enhanced Raman scattering properties are obtained after their combination. In order to have a comprehensive knowledge of these nanocomposites, this Review highlights the chemical and biological synthesis of Ag–graphene nanocomposites. In particular, their applications as antimicrobial agents, catalysts, and sensors in biomedicine, agricultural protection, and environmental remediation and detection are covered. Meanwhile, the factors that influence the synthesis and applications are also briefly discussed. Furthermore, several important issues on the challenges and new directions are also provided for further development of these nanocomposites.

1. Introduction

Graphene, an emerging 2D nanomaterial, has attracted tremendous attention due to its excellent properties, such as large surface area, high chemical stability, extreme mechanical strength, unique electronic, and thermal conductivity properties.[1–3] Since its discovery in 2004,[4] the number of researches on graphene has increased at an unexpected rate. Currently, the most of graphene nanomaterials used and studied are graphene oxide (GO) and reduced graphene oxide (rGO).[5] GO possesses abundant oxygen-containing functional groups, which provide the possibility for further chemical modification and functionalization. rGO is commonly obtained by the removal of oxygen-containing functional groups on GO with some reduction routes.[6,7] The detailed information on their structures and properties can be obtained from several reviews.[5–8] It has been reported that graphene nanomaterials have great application potential in various fields, such as supercapacitors,[9] solar cells,[10] sensors,[11] and catalysts,[12] etc. Until now, it is still being considered as a brightly shining star in material science horizon.[13] To utilize the fascinating properties and unique structure of graphene nanomaterials, considerable efforts have been made to develop graphene hybrid nanocomposites. Hitherto, graphene sheets have been developed as nanoscale building blocks to disperse and stabilize various metal and metal oxide nanoparticles (Ag, Au, Pt, Pd, Cu, ZnO, SnO_2, and TiO_2).[14–19] Importantly, some synergistic and novel properties of nanocomposites can be obtained after hybridization.[20] Therefore, graphene sheets as nanoparticle supports open up a new pathway for the material development.

Among those doped nanoparticles, silver nanoparticles (AgNPs) have attracted increasing interest due to their exceptional optical, electronic, catalytic, and antibacterial properties.[21–26] Since graphene can act as an efficient support material to disperse AgNPs and prevent their agglomeration, thus, the combination of AgNPs and graphene materials has received considerable attention to overcome their application limitations. More importantly, the combination can enhance surface enhanced Raman scattering (SERS), catalytic, and antibacterial properties in comparison with the individual component.[20,27–29] Furthermore, the size and loading of AgNPs can be controlled on graphene sheets, which are critical for the design and application of nanocomposites.[30,31] After the deposition of AgNPs onto graphene sheets (referred as Ag–GO and Ag–rGO nanocomposites), the new nanocomposites can exhibit special features, which will further promote their applications in optical

Dr. K. He, Prof. G. M. Zeng, Dr. P. Xu, Dr. Z. Z. Huang, Dr. J. B. Shi, Dr. L. Hu, Prof. G. Q. Chen
College of Environmental Science and Engineering
Hunan University
Changsha 410082, P. R. China
E-mail: zgming@hnu.edu.cn
Dr. K. He, Prof. G. M. Zeng, Dr. P. Xu, Dr. Z. Z. Huang, Dr. J. B. Shi, Dr. L. Hu, Prof. G. Q. Chen
Key Laboratory of Environmental Biology and Pollution Control
Ministry of Education
Changsha 410082, P. R. China
Dr. Z. T. Zeng, Prof. R. Xiao
Department of Dermatology
Second Xiangya Hospital
Central South University
Changsha 410011, P. R. China
E-mail: xiaorong65@csu.edu.cn
Dr. A. W. Chen
College of Resources and Environment
Hunan Agricultural University
Changsha 410128, P. R. China

DOI: 10.1002/smll.201800871

and electronic devices, catalysis, sensors, and antimicrobial agents.[32–34] As a result, enormous attention has been paid on the synthesis and applications of Ag–graphene nanocomposites. However, to our knowledge, the information on the synthesis and applications of Ag–graphene nanocomposites is rather scattered. Thus, an all-round overview of the synthesis and applications of Ag–graphene nanocomposites is necessary.

In order to have a comprehensive knowledge of Ag–graphene nanocomposites, the recent related reports are summarized in this Review. Specially, the main subjects are focused on various synthetic approaches including chemical and biological methods, and the applications as antimicrobial agents, catalysts, and sensors in many fields. In addition, the influence factors on synthesis and applications, synthetic mechanisms, and potential applications are also discussed. Herein, we deem that this Review will provide theoretical basis and valuable insights for the development of Ag–graphene nanocomposites. Meanwhile, the challenges and outlooks are also put forward to promote the development of Ag–graphene nanocomposites.

2. Synthesis of Ag–Graphene Nanocomposites

Great efforts have been made to explore the routes for the synthesis of Ag–graphene nanocomposites. The strategies for preparing Ag–graphene hybrid materials include the deposit method and in situ reduction method. In deposit method, AgNPs are prepared firstly and then deposited on GO sheets (Ag–GO nanocomposites) by physical absorption, electrostatic binding, or charge transfer interactions.[35–37] With further reduction of Ag–GO, the Ag–rGO nanocomposites can be obtained. The size and shape of AgNPs can be controlled in this method. However, time-consuming steps and complex manipulation are required.[36] To date, the in situ reduction of Ag^+ ions on graphene sheets has been widely applied for the synthesis of Ag–graphene nanocomposites due to its simple and effective large-scale production.[38–41] In this section, we will mainly discuss the in situ synthesis of Ag–graphene nanocomposites including Ag–GO and Ag–rGO nanocomposites via chemical and biological methods.

2.1. Chemical Methods

Chemical reduction is one of the most popular approaches for the synthesis of Ag–graphene nanocomposites.[42] Generally, the chemical reduction process is conducted in a solution system containing three main components: metal precursors, graphene oxide, and reductant. For the reduction of Ag^+ ions, various reductants such as borohydride,[32,41,43] sodium citrate,[44–46] ascorbic acid,[47] and dopamine[48] are used in the composite synthesis. In addition, stabilizing/capping agents are used to control particle growth in some cases.[20]

In 2009, Pasricha et al. prepared Ag–GO nanocomposites by utilizing the reducing nature of GO under alkaline conditions without any functionalization.[49] Wang et al. developed an approach to fabricate the shape-controllable silver materials (nanoparticles, nanocubes, and dendrites) on GO sheets by changing Ag^+ ions concentration, sampling orders and reaction times. In this method, GO played dual roles as substrate and reductant.[36] With the idea of reducing nature of GO, Ag–rGO composites were synthesized through a rapid one-pot strategy, which was conducted in sodium hydroxide solution at 80 °C for 10 min under stirring without the extra reductants and surfactants.[50] The results indicated that the amount of Ag^+ ions showed positive correlation with the size and density of formed AgNPs, and demonstrated that the Ag–rGO nanocomposites could enhance the photocurrent generation. Besides, the density of AgNPs played an important role in the photocurrent generation. Actually, large number of studies have been focused on the green and facile chemical methods for the synthesis of Ag–graphene nanocomposites. For example, glucose has been used as reducing and stabilizing agent to prepare Ag–GO nanocomposites. However, the dispersion of AgNPs is heterogeneous.[51] Yuan et al. fabricated graphene/Ag nanocomposites by using sodium citrate as reducing agent and found that the AgNPs were dispersed on graphene homogeneously. Furthermore, they found that the dosage of $AgNO_3$ was critical to control the size and shape of the AgNPs. In addition, the SERS and antibacterial properties could be retained.[52] Yang et al. employed TWEEN 80, a nonionic biocompatible surfactant, as the reducing and stabilizing agent of AgNPs and as modifier of GO to synthesize the AgNPs decorated TWEEN/GO composites. Meanwhile, they found that this as-prepared nanocomposites showed excellent electrochemical performance.[53] Zhang et al. prepared Ag–graphene nanosheets with a facile one-plot method by using poly-(*N*-vinyl-2-pyrrolidone) (PVP) as the

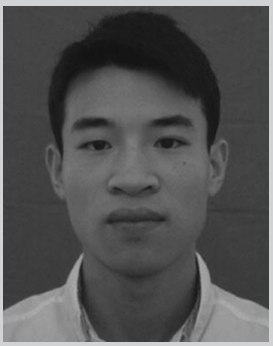

Kai He obtained his Master's degree in soil ecology from Southwest University, China in 2015. Now, he is pursuing his Ph.D. degree in the College of Environmental Science and Engineering at Hunan University, China. His research interests are focused on the preparation of functional graphene and clay materials, their applications in environmental remediation, and their environmental behaviors.

Guangming Zeng received his Ph.D. degree from Wuhan University in 1988. He has been the director of College of Environmental Science and Engineering at Hunan University since 1996. He is a Cheung Kong Scholar professor. He has been working in the fields of chemical biology, bionanotechnology, molecular engineering, and environmental pollution control.

reductant and stabilizer, and demonstrated that the adjustable sizes and well-controlled densities of AgNPs could be obtained by changing the reaction time and GO concentration. The average size of AgNPs increased with reaction time and the morphology of AgNPs gradually changed from spherical to irregular shapes with reaction proceeded. Furthermore, they found that graphene nanosheets were essential for intensifying the SERS signals.[20] Ag–GO nanocomposites could be prepared by in situ ultrasonication of a mixture solution of $AgNO_3$ and GO and vitamin C was used as reductant at room temperature. This study provided a guide for the synthesis of dimension-controlled AgNPs on GO surface. The dimensions of AgNPs increased with the increase of either ultrasonication time or the amount of $AgNO_3$.[54] Importantly, these studies pointed out the parameters for controlling the size and density of AgNPs on graphene sheets, which are vital for optimizing the properties of Ag–graphene nanocomposites.

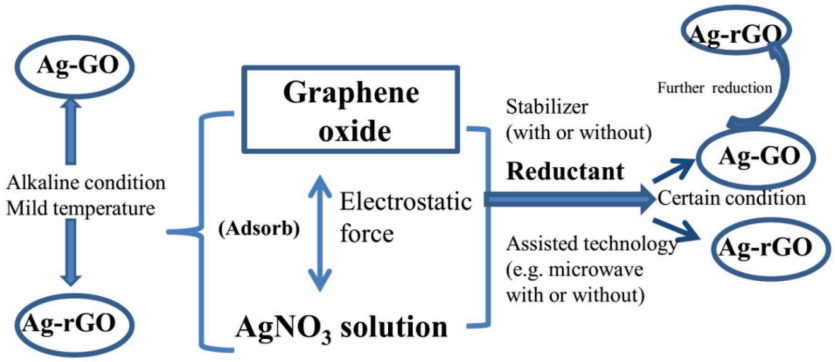

Figure 1. The synthetic processes and mechanisms of Ag–GO and Ag–rGO nanocomposites.

Ag–rGO nanocomposites are generally prepared in two steps, including the reduction of Ag^+ ions on GO sheets and the further reduction of GO.[32,49,55] In order to simplify the operating procedures, one-pot synthesis of Ag–rGO has been proposed. For instance, Shen et al. prepared Ag–rGO nanocomposites by one-pot hydrothermal reaction with ascorbic acid as reductant.[47] Tang et al. developed a one-step route to prepare Ag–graphene nanocomposites by the simultaneous reduction of GO and Ag^+ ions with formaldehyde as reducing agent.[56] Tannic acid (TA), a water-soluble phenolic hydroxyl-rich compound which is widely present in woods, has been reported as reducing agent to prepare Ag–graphene nanocomposites in one-pot route. The as-prepared nanocomposites exhibited excellent SERS and electrochemical properties.[57] However, the reduction abilities of above-mentioned reductants are relatively weak.[58] To date, several efficient technologies have been applied to further shorten the reaction time. A rapid one-pot synthesis of Ag–rGO hybrids was proposed by using sodium citrate as green reductant with the help of microwave irradiation (MWI). Herein, MWI can provide higher energy efficiency to shorten the reaction time in comparison with other traditional heating methods, which can reduce the required time and energy in the preparing process. The resultant nanocomposites with spherical AgNPs (20 nm) exhibited excellent electromagnetic interference (EMI) shielding performance.[58] Liu et al. reported a rapid one-pot, microwave-assisted preparation of AgNPs/GN composites with dimethylformamide (DMF) as solvent and reducing agent.[59] Furthermore, photochemical synthesis method has been demonstrated as an effective and green method for the preparation of Ag–graphene nanocomposites. In this strategy, the formation of AgNPs was triggered by illumination without additional reductant and surfactant.[60] Similarly, infrared light-assisted preparation of Ag–rGO nanocomposites were successfully obtained by the reduction of GO and Ag^+ ions.[61] These technologies will promote the large scale production and application of Ag–graphene nanocomposites.

According to the above-mentioned reports, the main factors that influence the size and shape of AgNPs in the nanocomposite synthesis may include the amount of Ag^+ ions, GO concentration, and reaction time. Besides, the selected reductants also influence the synthesis of nanocomposites. The synthetic process is schematically described in **Figure 1**. Commonly, the negatively charged oxygen-containing functional groups on the surface of GO will bind with Ag^+ ions via electrostatic force, and then the AgNPs are deposited on graphene sheets by reduction.

2.2. Biological Methods

Biological methods for the synthesis of Ag–graphene nanocomposites are becoming increasingly popular. In 2015, Khan et al. first reported a biogenic method, which can reduce the use of harsh chemicals, on the synthesis of Ag–graphene nanocomposites by using an electrochemically active biofilm (EAB) as reducing tool. The resultant composites with spherical AgNPs (10–30 nm) on the surface of graphene sheets exhibited enhanced photocurrent and photocatalytic performance.[62] Sreekanth et al. synthesized Ag–GO nanosheets using the aqueous extract of dry jujube fruit extract as capping and reducing agent.[63] However, the shape of AgNPs was predominantly spherical, triangular, and uneven in shape, indicating the difficulties to control particle shape with this method. In another study, Ag–GO nanosheets were prepared by using *Picrasma quassioides* bark aqueous extract as reducing and capping agent, which showed high catalytic activity.[64] Shaikh et al. reported a one-step synthesis of Ag–rGO nanocomposites by phytoreduction with excellent electrocatalytic activity. Here, *Justicia adhatoda* (adulsa) leaf extract as green reducing agent could simultaneously reduce Ag^+ ions and GO. Meanwhile, it could also act as effective capping agent.[30] Although biological methods are still at early stage, they have great potential to efficiently synthesize Ag–graphene nanocomposites.

To our knowledge, Ag nanoparticles are mainly decorated on the surface of graphene in the above reports. In view of the chemical instability of silver, some researchers have explored the approaches by encapsulating or passivating Ag surfaces to retain its excellent properties. For instance, Jiang et al. reported a fabrication of GO wrapped Ag nanomushroom with seed-mediated synthesis method, which showed a more stable SERS performance after exposure to air for one month as compared

with the unwrapped one.[65] Chen et al. fabricated GO encapsulated AgNPs (Ag@GO) hybrid materials by the interaction of presynthesized Ag–NH_2 and GO–COOH solution. They suggested that the as-prepared Ag@GO composites as SERS probe exhibited three advantages including: 1) GO shell can prevent the oxidation of Ag nanoparticles, thus enhancing the chemical stability; 2) GO provides efficient adsorption sites; 3) the oxygen-containing functional groups on GO make this hybrid material suitable for further functionalization.[66] Reed et al. fabricated Ag nanoantennas with a layer of graphene (0.355 nm thick), which could serve as an excellent protective layer without detrimental effect, on the top to prevent the Ag sulfidation.[67] Consequently, more attention should be paid to these approaches to optimize and enhance the properties of these nanocomposites.

3. Antimicrobial Agents

With the increase of microbiological contamination and infection in environment, ecosystem, and human, the removal and destruction of harmful microbes have become an urgent topic for the health and development of human being.[68] Because of the excellent broad-spectrum antimicrobial activity, AgNPs as antimicrobial agents have been gained abundant attention.[69–71] In addition, large number of papers have reported the potential antibacterial properties of graphene and its derivatives.[72–74] Those findings further show the great application potential of Ag–graphene nanocomposites as ideal antimicrobial agents.[75] Based on the numerous reports below, Ag–graphene nanocomposites as antimicrobial agents can be applied in biomedicine, waster disinfection, and plant disease management.

3.1. Antimicrobial Performance

The broad-spectrum antimicrobial activity of Ag–graphene based nanocomposites has been reported by numerous studies. For example, GO–Ag nanocomposites exhibited excellent antibacterial activity against methicillin-resistant *Staphylococcus aureus* (MRSA), *Acinetobacter baumannii*, *Enterococcus faecalis*, and *Escherichia coli* (*E. coli*).[76] Barua et al. prepared a biocompatible antimicrobial rGO–AgNPs nanohybrid and found that the minimum inhibitory concentrations (MIC) and inhibitory zones of this nanohybrid against *E. coli* (20 μg mL^{-1}, 18.84 mm), *S. aureus* (12.5 μg mL^{-1}, 23.82 mm), and *Candida albicans* (6 μg mL^{-1}, 21.73 mm) were superior to the individual nanomaterials.[77] Geetha Bai et al. reported that reduced graphene oxide-silver (rGO-Ag) nanocomposites exhibited a comparable antibacterial activity to the standard antibiotic, chloramphenicol.[75] Ma et al. found that Ag–GO nanosheets displayed excellent antibacterial properties toward *E. coli*. Meanwhile, cell deformation was observed after *E. coli* was treated with Ag–GO nanosheets.[78] Jiang et al. prepared a novel Ag/graphene nanocomposite with well dispersed AgNPs (45–50 nm) onto graphene sheets. They investigated their antibacterial activity against *E. coli* using the agar well diffusion method and found that the average diameter of inhibitory zones for *E. coli* was 18.65 mm. As a result, they suggested that

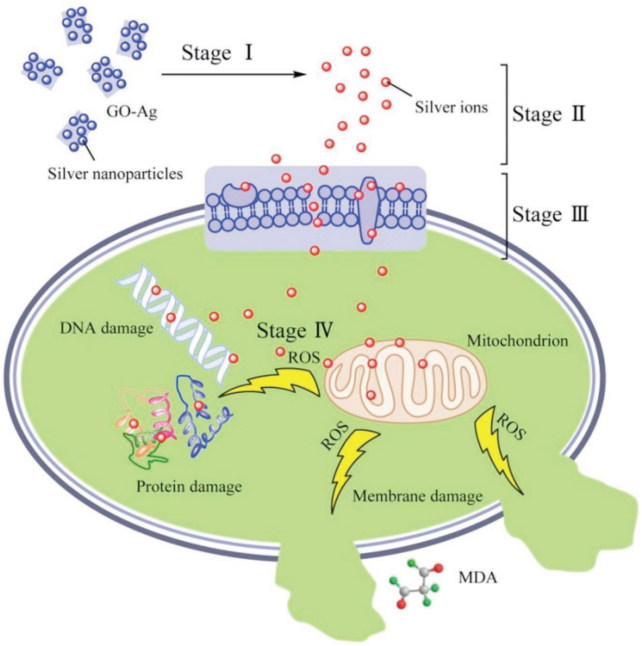

Figure 2. Schematic mechanisms for antibacterial behaviors of GO–Ag nanocomposites. Blue dots represent silver nanoparticles loaded on GO sheets, and red dots are silver ions. The roman numerals (I, II, III, and IV) refer to different stages of the bactericidal process. Reproduced with permission.[81] Copyright 2016, Elsevier Inc.

the outstanding inhibitory property should be attributed to the good dispersibility of AgNPs and introduction of high-quality graphene.[79] He et al. investigated the antibacterial activity and mechanism of graphene-based silver nanoparticles (AgNPs-GE, 10 nm AgNPs) on *Pseudomonas aeruginosa* (*P. aeruginosa*), a common Gram-negative nonfermenting bacterium that is ubiquitous in the hospital environment. The results showed that the MIC and minimum bactericidal concentration (MBC) values of AgNPs-GE were 5 and 20 μg mL^{-1}, respectively. The pathway in antibacterial action of AgNPs-GE was related to the inhibition of translation.[80] Song et al. suggested that the antibacterial behaviors of GO–Ag nanocomposites were involved in multiple stages including the destruction of cell membranes and oxidative stress as shown in **Figure 2**.[81] Shao et al. reported the low cell cytotoxicity and excellent antibacterial activity of GO–Ag nanocomposites (22 nm AgNPs). In their study, the antibacterial ratio increased with the increasing dosage of GO-Ag nanocomposites and the antibacterial effect was better against *E. coli* than *S. aureus* at the identical condition.[82] Das et al. found that *P. aeruginosa* was comparatively more sensitive to the Ag–GO suspension compared with *E. coli*.[83]

Obviously, Ag–graphene nanocomposites displayed different antibacterial activities against different bacteria (**Table 1**). The differences in antibacterial activities may be ascribed to the differences of cell wall structures (i.e., permeability and structural integrity of bacteria membranes). Generally, the transfer of the external materials from solution to the membrane will be affected by the peptidoglycan layer in the cell walls. Thus, the different peptidoglycan layer thickness in the cell walls between Gram-positive bacteria and Gram-negative bacteria will cause the different antibacterial activities.[75,84,85] Nonetheless, the

Table 1. The antibacterial activity of Ag–graphene based nanocomposites on different bacteria.

Graphene type	AgNPs size [nm]	Bacteria	Bacteria concentration (dosage)	Measurement method	Antibacterial rate [%]	Inhibition zone [mm]	MIC (MBC) [μg mL^{-1}]	Reference
Graphene	45–50	*Escherichia coli*	(20 μL, 100 μg/μL)	Agar well diffusion		18.65		[79]
Graphene oxide	≈10	*Pseudomonas aeruginosa*	10^7 cfu mL^{-1}, 20 mL (0–35 μg mL^{-1})	Optical density			5 (20)	[80]
Graphene oxide	5–15	*Escherichia coli*	10^5–10^6 cfu mL^{-1}, 25 mL (40–280 mg L^{-1})	Plate colony-counting	89.72–99.99			[81]
		Staphylococcus aureus			70.32–97.65			
Graphene oxide	46	*Escherichia coli*		Plate colony-counting			4	[86]
		Staphylococcus aureus					14	
Graphene oxide	9.4 ± 2.8	*Staphylococcus aureus*	1.5×10^5 cfu well^{-1} (60–1.0 μg mL^{-1})	Microdilution assay			15 (30)	[76]
Reduced graphene oxide	15–20	*Staphylococcus aureus*	10^6 cfu well^{-1} (1–40 μg mL^{-1})	Agar well diffusion/ microdilution assay		23.82 ± 0.18	12.5	[77]
		Escherichia coli				13.88 ± 0.06	20	
		Candida albicans				21.73 ± 0.13	16	
Graphene oxide	–	*Escherichia coli*		Plate colony-counting	100			[78]
Graphene oxide	22	*Escherichia coli*	4×10^6 cfu mL^{-1} (60 μL, 20 μg mL^{-1})	Plate colony-counting	98.36			[82]
		Staphylococcus aureus			96.18			
Graphene oxide	80	*Escherichia coli*	10^5–10^6 cfu mL^{-1}, 150 mL (45 mg L^{-1})	Plate colony-counting	100			[85]
		Staphylococcus aureus			86.6			
Reduced graphene oxide	6.02 ± 0.31	*Escherichia coli*		Agar well diffusion		14.00	<62.5 (>1000)	[75]
		Pseudomonas aeruginosa				–	125 (1000)	
		Staphylococcus aureus				13.00	<62.5 (500)	
		Bacillus cereus				3.33	1000 (>1000)	

above-mentioned studies did not clarify the antibacterial action modes against different bacteria. To understand their effects on different bacteria, Tang et al. carried out an experiment on Gram-negative bacteria *E. coli* and Gram-positive bacteria *S. aureus*. As a result, they found that the antibacterial effects of GO-AgNPs were species-specific dependent. GO-AgNPs damaged *E. coli* by inducing the disruption of cell integrity, whereas it killed *S. aureus* by dramatically inhibiting cell division, which could be observed from confocal fluorescent images (**Figure 3**). Meanwhile, they suggested that antibacterial activity of GO-AgNPs was attributed to the synergistic antibacterial effect rather than the additive effect of bare GO and AgNPs.[86] Overall, Ag–graphene nanocomposites show better antibacterial activity than the individual nanomaterials, and the antibacterial mechanisms include the chemical and physical damages as mentioned above.

The assembly of other compounds or nanoparticles, which have the bactericidal effect or special functions such as detection and separation, into Ag–graphene nanocomposites have been regarded as an efficient approach to enhance their antibacterial activity.[87–92] According to the combined biological inhibitory activities of GO, aminophenol, and AgNPs, Pant et al. developed an aminophenol grafted and AgNPs decorated reduced graphene sheet (Ag–RGS) as a promising antibacterial agent against *E. coli* and *S. aureus*.[87] Chitosan is

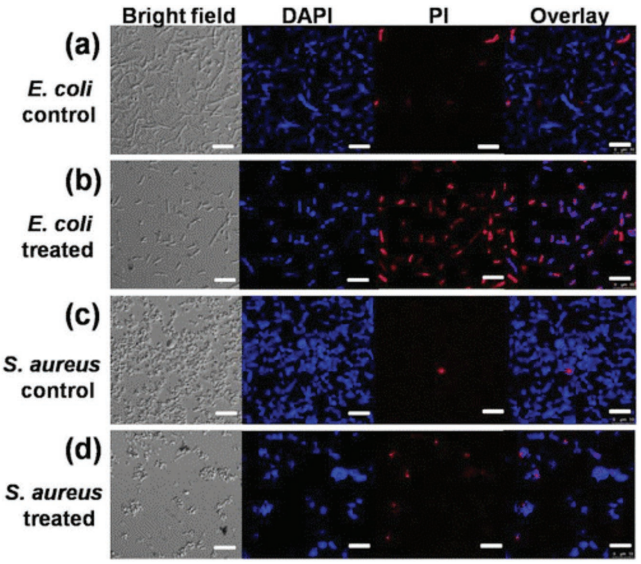

Figure 3. Confocal fluorescent images of live and dead bacterial cells after incubation with 10 μg mL^{-1} of GO-Ag nanocomposite (Ag:GO=1:1) for 2.5 h: a) *E. coli* no treatment; b) *E. coli* with nanocomposites; c) *S. aureus* no treatment; d) *S. aureus* with nanocomposites. Blue fluorescence shows bacterial quasi nuclear stained with DAPI, while red fluorescence shows dead bacteria stained with PI. The scale bar is 10 μm. Reproduced with permission.[86] Copyright 2013, American Chemical Society.

a biocompatible polymer, which can not only exhibit a strong bactericidal and homeostatic effect, but also act as coating agent to increase the stability of nanoparticles.[88,89] Marta et al. investigated the antibacterial activity of chitosan–silver nanoparticles–GO (chit–AgNPs–GO) nanomaterial against *S. aureus*, and suggested that adsorption properties of chitosan could maximize the interaction of chit–AgNPs–GO with cells through a capturing-killing process.[90] Copper nanoparticles (CuNPs) have been reported to exhibit bacterial toxicity and were used to assemble GO–Cu–Ag nanocomposites.[91] The bactericidal effect of GO–Cu–Ag was more effective than that of individual nanoderivatives (CuNPs, AgNPs, and Cu-AgNPs), which was attributed to the morphological diversity of nanoparticles and GO that could synergistically attack cells.[91] Naskar et al. confirmed the effective antibacterial activities of Ag–ZnO–graphene nanocomposites against *E. coli* and *S. aureus* without damage on the surrounding cells.[92] In 2017, Roy et al. developed a molecularly imprinted polymer (MIP) modified Ag–ZnO bimetallic nanoparticles to decorate GO nanocomposite through the combination of molecular imprinting with photothermal method. Their study indicated that the quantitative estimation, capture, removal, and photothermal destruction of *E. coli* were rapid and sensitive by this nanocomposite. This design provided a three-in-one kit for bacteria (detection, removal, and killing; DRK), which was convenient for the on-site application in real water and food samples.[93] In addition, the loading of magnetic nanoparticles onto Ag–graphene nanocomposites has gained wide attention as well, owing to their exception properties of magnetic separation and bacterial inactivation.[94] It has been reported the easy separation and high antibacterial activity of AgNP-decorated magnetic GO (MGO-Ag) against *E. coli* and *S. aureus*.[95] Therefore, it is necessary to explore additional improvement approaches and technologies to promote the practical application of Ag–graphene based nanocomposites as antimicrobial agents.

3.2. Biofouling

Biofouling is a serious problem in separation/desalination membrane process for water purification.[96] To improve the anti-biofouling properties of membranes, Ag–graphene nanocomposites have been used as membrane antibacterial agents. For example, Li et al. reported that GO–Ag modification could improve the hydrophilicity, mechanical property, and permeability of polyvinylidene fluoride (PVDF) membrane. Importantly, the modified PVDF membrane exhibited significant antibacteria adhesion property and inhibition on biofilm formation. Meanwhile, the presence of GO could efficiently prevent the release of Ag^+.[97] Likewise, GO–Ag modified cellulose acetate (CA) membrane also exhibited strong antibacterial activity, as the inhibitory efficiency of *E. coli* growth reached 86% for 2 h and nearly 100% for 4 h.[98] GO–Ag sheets modified thin-film composite (TFC-GOAg) exhibited a 80% inactivation rate on the growth of *P. aeruginosa* and significantly suppressed the biofilm formation.[99] In another study, GO/Ag modified TFC polyamine membrane exhibited super-hydrophilic property and significant inactivation rate against *E. coli* (over 95%). Meanwhile, GO–Ag modification did not affect the transport property of membrane.[100] The surface modification of membrane with Ag–graphene nanocomposites provides an effective approach to control the biofouling in membrane filtration, thereby increasing the sustainability of membrane technologies for water purification.

3.3. Plant Protection

With the rapid development in nanotechnology, the combination of engineered nanomaterials with biotechnology is increasingly popular. Nowadays, Ag–graphene based antimicrobial agents have been applied in plant protection and nutrition. For example, Ocsoy et al. developed DNA-directed AgNPs that grown on GO (Ag@dsDNA@GO) composite as an antibacterial agent against *Xanthomonas perforans*, a model plant pathogenic bacterium that can cause serious bacterial spot disease of tomatoes. Compared with Ag@GO, Ag@dsDNA@GO showed higher antibacterial activity, owing to the increased adhesive force between Ag@dsDNA@GO composites and bacterial cell membranes in the presence of dsDNA. More importantly, the application of Ag@dsDNA@GO could not cause the phytotoxicity on leaves.[101] In 2016, Chen et al. investigated the antifungal activity of GO–AgNPs nanocomposites against phytopathogen of *Fusarium graminearum* (*F. graminearum*), which can cause *Fusarium* head blight (FHB) disease in wheat plants, in vitro and in vivo for the first time. Their results showed that GO–AgNP nanocomposites significantly inhibited the germination of spores and the development of germ tubes of *F. graminearum*. After spraying with GO–AgNP nanocomposites (6.85 and 7.81 μg mL^{-1}), the hyphae changed from normal smooth, intact and slender bodies to the sunken and stacked structure. Furthermore, macroconidia became crumpled, wizened, and stacked that was obviously different from the typical slender, sickle-shape morphology. The detached leaf experiment showed that the leaf spot disease reduced significantly after spraying GO–AgNP on wheat leaves. In addition, they found that both the physical damage on biological structure and oxidation stress on cells were the inactivation mechanisms to control the disease development.[102] The detailed antifungal characterization of GO–AgNP nanocomposites is shown in **Figure 4**. These findings collectively manifest the great application potential of Ag–graphene nanocomposites in the agricultural production.

4. Catalysts

4.1. Catalytic reduction

The reduction of nitroarenes to anilines is one of the highly important organic transformations.[103] For example, 4-nitrophenol (4-NP) has been listed as a "priority pollutant" by the US Environmental Protection Agency (EPA).[104] Its reduction to 4-aminophenol (4-AP) by $NaBH_4$ with Ag–graphene as catalyst has attracted particular interest in both environmental and industrial fields.[29,105,106] Ag–GO nanocomposites with 3.3% Ag content could be employed as highly effective and recyclable catalysts for the reduction of 4-NP by $NaBH_4$. After

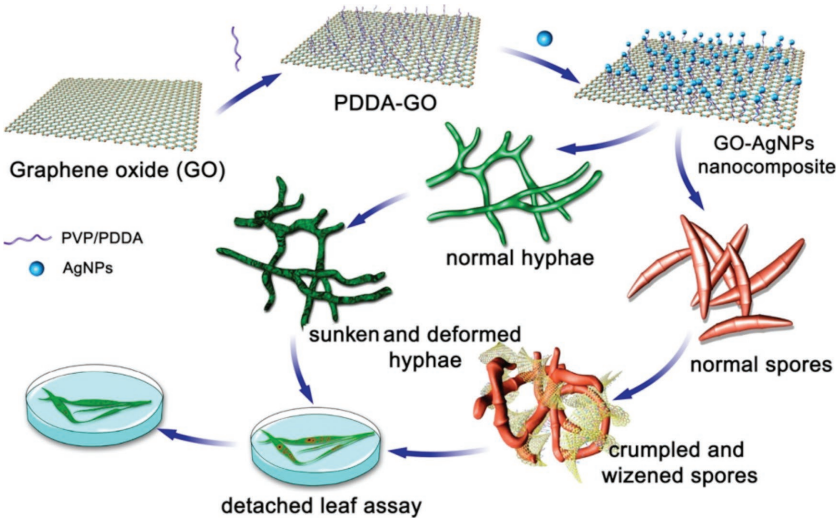

Figure 4. Schematic illustration of fabrication of GO–AgNPs nanocomposite and its antifungal characterization in vitro and in vivo. Reproduced with permission.[102] Copyright 2016, American Chemical Society.

seven successive cycles of reduction, the reduction efficiency still remained at 86.2%.[105] AgNPs immobilized on poly(*N*-vinyl pyrrolidone)-grafted GO (GO-PNVP) as catalysts for the reduction of 4-NP into 4-AP by $NaBH_4$ showed efficient catalytic activity and excellent reusability.[29] Meng et al. also found that Ag/rGO nanocomposites showed high catalytic activity toward hydrogenation of 4-NP. And no obvious loss of activity was observed after three catalysis cycles.[107] In addition, Ag/rGO/TiO_2 nanocomposite was highly active for the reduction of 4-NP.[39] Paul et al. employed Ag/Fe_2O_3 decorated rGO (Ag/α-Fe_2O_3–rGO) as magnetically recoverable catalyst for the reduction of ten kinds of aromatic nitro groups to the corresponding amine, which showed high conversion efficiency (92–98%).[108] The superior catalytic activity of Ag–graphene nanocomposites on the reduction of 4-NP was attributed to π–π stacking between 4-NP and graphene sheets, which could cause a high concentration of 4-NP near to AgNPs, thereby facilitating the catalytic reduction.[107]

4.2. Photocatalytic Degradation

Photocatalysis is an evolving technology for decomposing organic contaminants in environment.[109,110] AgNPs are important materials in photocatalysis, owing to their unique plasmon resonance that can enhance the light-absorption capability.[111] Graphene has already been used as a conducting support for AgNPs.[112] The utilization of Ag–graphene based nanocomposites for photocatalysis has been carried out. For example, Meng et al. synthesized Ag–rGO nanocomposites by one-step hydrothermal method and found that this as-prepared nanocomposites showed promising photodegradation toward Rhodamine B (RhB).[113] Khan et al. reported a biogenic synthesis of Ag–graphene nanocomposite with hydrophilic nature, which exhibited efficient photocatalytic degradation toward Methylene blue (MB) and Congo red (CR) dyes under visible-light irradiation. Meanwhile, they suggested that the loading of low concentration of AgNPs enhanced the visible light harvesting and increased the charge carrier mobility.[62] Hareesh et al. found that the degradation of MB using Ag–rGO as photocatalyst reached 99.71% for the first cycle and remained 92.89% even after 8th cycle.[114]

In addition, AgNPs can be used as bridges and skeletons between other photocatalysts and graphene materials, due to their high electron capture capacity. The incorporation with AgNPs can decrease the recombination of photogenerated electron/hole (e^-/h^+) pairs, thus enhancing the photocatalytic activity.[115–117] For example, Ag/TiO_2/graphene exhibited highly efficient photocatalytic decolorization toward MB dye.[118] In another study, Ag/TiO_2/rGO was synthesized by a combined sol–gel/solvothermal method in ethanol solution, which could photocatalytically decompose more than 79% of MB after 4 h of visible light irradiation, whereas only 35%, 38%, and 53% of MB were removed by TiO_2, Ag/TiO_2, and TiO_2/rGO photocatalyst, respectively.[119] rGO/Ag/TiO_2-nanotubes/Ti plate exhibited significantly enhanced photocatalytic activity for the photocatalytic degradation of MB dye as compared with TiO_2-nanotube plate under UV light irradiation.[115] The degradation of RhB by Ag and graphene (GR) codoped monoclinic $BiVO_4$ ternary systems (Ag/GR/$BiVO_4$) outperformed binary systems of Ag/$BiVO_4$ and GR/$BiVO_4$ as well as solitary $BiVO_4$, which was ascribed to the cooperation among AgNPs, graphene sheets, and cuboid-shaped $BiVO_4$ that could enhance quantum efficiency and extend light response range.[120] Similarly, Ag and graphene comodified Bi_2WO_6 nanosheets (Ag–G-Bi_2WO_6) exhibited high photocatalytic degradation of RhB under visible light irradiation.[111] A high-efficiency degradation of Direct Green BE under UV–vis light was observed using Ag/$LaMnO_3$–graphene as photocatalyst.[117] Furthermore, the removal of organic pollutants can be further enhanced by photocatalysis when combining with other advanced oxidation process (AOP) such as electrochemical oxidation.[121] Commonly, their combination is known as photoelectrochemical process. Umukoro et al. have reported the higher photoelectrochemical removal efficiency on orange II dye degradation by Ag–ZnO–rGO (93%) as a photoanode material than that by ZnO–rGO (87%) and rGO (73%) electrodes.[121]

In addition to organic dyes, the photodegradation of colorless organic pollutants by Ag–graphene based nanocomposites is another important subject. Bhunia and Jana demonstrated that rGO–Ag could be used as photocatalyst for the degradation of colorless endocrine disruptors (phenol, bisphenol A, and atrazine) under visible light.[122] The proposed degradation mechanism is shown in **Figure 5**. Meanwhile, they suggested that the optimum Ag loading was vital for controlling photoexcited electron/hole pairs.[122] Likewise, Liu et al. also found that low and high contents of Ag were not suitable for the photocatalytic degradation of phenol.[123] Cui et al. found the enhanced photocatalytic activity of Ag_3PO_4/rGO/Ag heterostructural photocatalyst for the degradation of MB and phenol.[124] In

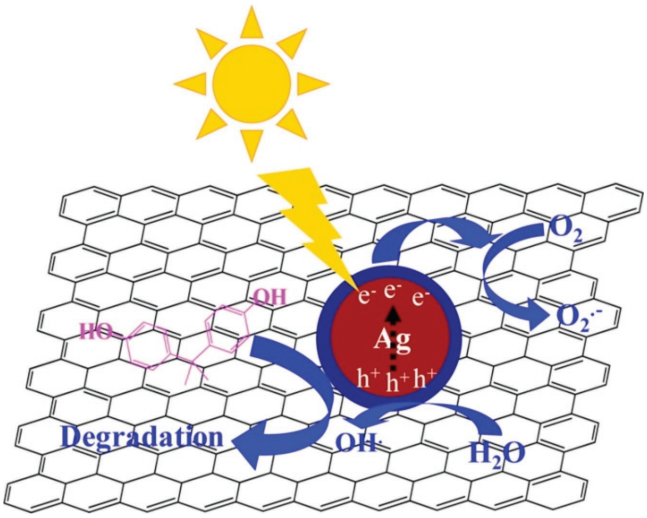

Figure 5. Proposed mechanism for photocatalytic degradation of endocrine disruptors by rGO–Ag catalyst under visible light. Reproduced with permission.[122] Copyright 2014, American Chemical Society.

2015, Yu et al. found that metoprolol (10 μg mL^{-1}, 50 mL), one of pharmaceuticals and personal care products (PPCPs), was completely eliminated after 2 h of simulated solar light irradiation using Ag–Bi_2WO_6–graphene (1 mg mL^{-1}) as photocatalyst, which was significantly enhanced as compared with pure Bi_2WO_6.[125]

According to the above-mentioned studies, an optimum Ag content on the composites is critical for the photocatalytic degradation. Because the excess AgNPs on the material surface would inevitably cover active sites and inhibit light adsorption, thus causing the decrease of photocatalytic activity. Whereas low loading of AgNPs could not provide sufficient reactive oxygen species to degrade organic pollutants.[122–124] Thus, the load of Ag content is important for the final photocatalytic performance. Graphene can provide strong adsorption ability of aromatic molecules due to π–π stacking and AgNPs are electron capture agent that can lead to fast photogenerated charge separation, thus the synergistic effects of Ag and graphene can enhance photocatalytic activity.[111,118,126] Overall, the Ag–graphene based nanocomposites could be used as excellent photocatalysts for the degradation of various organic dyes and colorless organic pollutants.

5. Sensors

The application of nanomaterials as sensors have attracted widespread attention in sensoring areas.[127–129] To date, Ag–graphene based nanocomposites are increasingly prevalent as sensors.[20,28] Owing to their intrinsic important features, AgNPs decorated on graphene surface could increase SERS activity, electrocatalytically active surface area, and stability, making them excellent in sensoring areas.[28,53] It has been reported that the applications of Ag–graphene based nanocomposites in chemical and biological sensoring are ultra-sensitive, time-saving, and cost-effective.[130–132] In this section, we mainly highlighted the detection performance of various Ag–graphene based nanocomposites as well as influence factors on the detection.

5.1. Chemical Sensoring

Efficient detection of various toxic or hazardous chemical substances, such as organic contaminants, heavy metals, and gas in environment, is important for ensuring our daily life. For the trace detection of organic aromatic molecules, so far, SERS has been proven to be an ultrasensitive and powerful analytical technique with high sensitivity.[28,132,133] Two SERS mechanisms including electromagnetic mechanism (EM) and chemical mechanism (CM) are generally accepted. EM is based on the enhancement of localized electromagnetic field that originates from the localized surface plasmon resonances (LSPRs) of noble metal nanoparticles.[132,134] CM is thought to originate from the charge transfer between absorbed molecules and metal surface.[28] As is well known, graphene sheets show efficient adsorption toward aromatic molecules due to π–π interactions, which can enhance the charge transfer, thus generating strong chemical enhancement.[132] Importantly, compared to the individual component, higher SERS signals arising from graphene/Ag hybrid structures could be observed. For instance, SERS signals of probe molecules such as RB and MB were shown to be significantly enhanced when compared with those of pure metallic nanoparticles. And a low detection limit of graphene/Ag hybrid could reach nanomolar (n M) levels.[133] SERS signals could still be detected from Ag octahedron@GO hybrid nanostructures at a detection limit for Rhodamine 6G (R6G) down to 0.1×10^{-9} M, which was two orders of magnitude lower than that of pure Ag octahedra.[132] Likewise, Huang et al. also found the enhanced SERS signals for the detection of organic dyes. Meanwhile, they suggested that the distribution and density of AgNPs governed the SERS performance.[28] Similarly, Zhang et al. found that the density of AgNPs on the surface of graphene could influence the SERS signal intensity as well.[20] In addition, a high SERS activity of functional graphene/silver (FG/Ag) nanocomposites was observed for the detection of *p*-aminothiophenol (PATP) and melamine.[135] 2,4,6-trinitrotoluene (TNT), a nitroaromatic explosive material, could be detected by using PATP-functionalized AgNPs supported on graphene nanosheets (Ag/GNs) as chemosensor, which showed high SERS sensitivity and selectivity. However, other structurally similar nitroaromatic compounds (NACs) such as nitrobenzene (NB), 2-nitrotoluene (2-NT), 4-nitrophenol (4-NP), and 2,4-dinitrotoluene (DNT) showed much weaker enhancements as compared to TNT at identical condition, owing to the reduction of effective charge transfer on the reduced nitro groups.[136] The two proposed SERS mechanisms for TNT detection is shown in **Scheme 1**. A and B represent the parallel and perpendicular model that molecules are adsorbed on the graphene sheets, respectively. The formed π conjugated structures may facilitate the charge transfer, thereby leading to the enhanced Raman signals.

Recently, a chemically modified electrode with Ag–graphene based nanocomposites has emerged as an efficient and versatile electrochemical sensor for the detection of NACs based on the excellent electrocatalytic activity.[137] Lu et al. reported

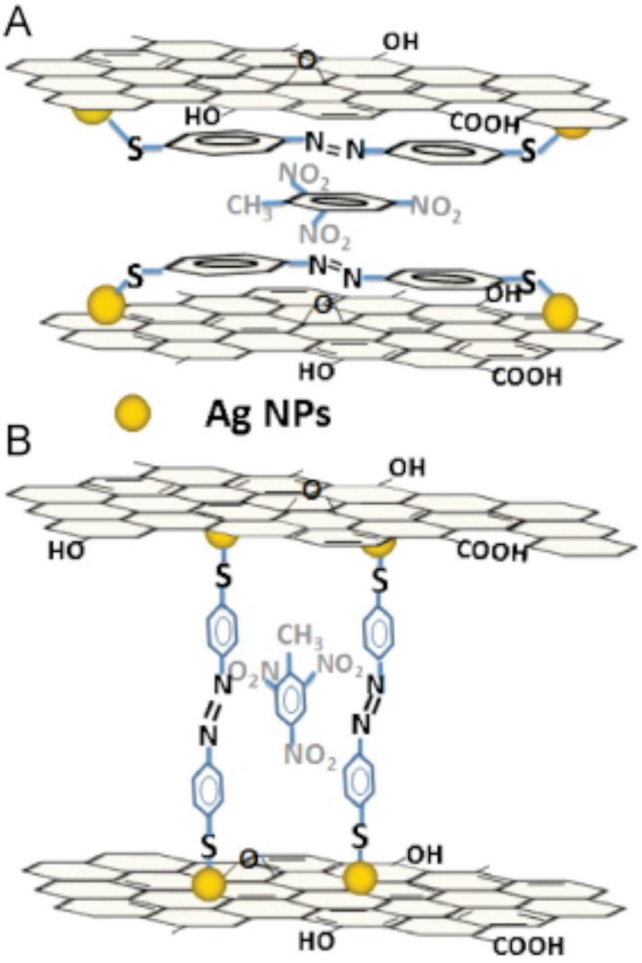

Scheme 1. SERS mechanisms for 2,4,6-trinitrotoluene (TNT) detection on the PATP modified Ag/GNs platform. Reproduced with permission.[136] Copyright 2013, Elsevier B.V.

a uniform carboxylic sodium functionalized graphene supported AgNPs (AgNPs/CS-G) with a lower detection limit of NB, DNT, and TNT of 0.60, 0.21, and 0.45 ppm, respectively.[137] Similarly, NB detection using rGO-AgNPs modified electrode as sensor has been successfully achieved with a detection limit of 0.261×10^{-6} M, detection sensitivity of 0.836 μA μM^{-1} cm^{-2}, and linear response range from 0.5 to 900×10^{-6} M, which was better than other modified electrodes (AgNPs and rGO).[35] Liu et al. reported the synthesis and application of β-cyclodextrin functionalized graphene/Ag nanocomposite (β-CD/GN/Ag) for the sensitive determination of 4-NP. A wide linear response to 4-NP in the ranges of 1.0×10^{-8} to 1.0×10^{-7} M and 1.0×10^{-7} to 1.5×10^{-3} M was achieved with a low detection limit of 8.9×10^{-10} M.[138] Furthermore, Dar et al. reported the application of AgNPs-GO modified glassy carbon electrode (AgNPs-GO/GCE) for arsenic(III) detection, which exhibited a wide linear range ($(13.33–375.19) \times 10^{-9}$ M) and a high sensitivity (180.5 μA μM^{-1}) with a detection limit of 0.24×10^{-9} M.[139] Shaikh et al. constructed Ag–rGO as nitrite (NO_2^-) sensor and found that this sensor exhibited two linear ranges: one from 10×10^{-9} to 1000×10^{-9} M with a sensitivity of 3.0×10^4 μA mM^{-1} cm^{-2} ($R = 0.999$) and another from 10×10^{-6} to 1000×10^{-6} M with a sensitivity of 373.46 μA mM^{-1} cm^{-2} ($R = 0.978$), with a sensitive detection below 1 ppm.[30] Wang et al. found that Ag nanoplates (AgP) on polyethyleniminemodified rGO (AgP/PEI-rGO) could be used as promising electrochemical sensor for detecting chloride ions (Cl^-), N_2H_4, and $NaNO_2$. Importantly, the modified electrodes still showed good detection performance even in the interference of some inorganic ions and organic materials.[140] Ag–graphene based composites also can be used as gas sensors.[141–144] For example, Uddin's group fabricated different Ag–ZnO–rGO hybrids for the efficient detection of acetylene (C_2H_2) with good selectivity and performance.[141,144] Tran et al. found that rGO sheets coated silver nanowires (rGO/AgNWs) showed better sensitivity to NH_3 than rGO/AgNPs.[142] Thus, it is necessary to further explore the roles of Ag nanostructures in sensors. Nonetheless, these results demonstrate the suitability of electrochemical method with the Ag–graphene based nanocomposites for the determination of various pollutants in environment.

5.2. Biological Sensoring

The use of nanomaterials as signal amplifiers has been successfully achieved for detecting biomolecules and bacterial cells,[145] which promotes the biosensor development. According to previous reports, Ag–graphene based nanocomposites can be used as efficient biosensors for the detection of biomolecules and bacterial cells. For example, Lu et al. reported a glucose biosensor (GOD immobilized on AgNPs-decorated functional-SiO_2/GO) with low detection limit of 310×10^{-6} M but without ideal stability.[133] In another work, the long-term stability of fabricated glucose biosensor was unsatisfactory (<5 days) as well.[57] Excitingly, much work has been carried out to improve the stability of biosensor efficiently.[146,147] Gupta et al. developed a novel glucose biosensor by immobilizing GOD on mercaptophenyl boronic acid (MBA) terminated Ag@AuNPs/GO (Ag@AuNPs-GO) nanomaterials (GOD-MBA-Ag@AuNPs-GO) with excellent detection performance and good stability, as no obvious change in the SERS spectrum was observed over 30 days.[146] Omidinia et al. fabricated a high sensitive L-phenylalanine (L-phe) biosensor by immobilizing phenylalanine dehydrogenase (PDH) onto rGO supported AgNPs hybrids (PDH-AgNPs/rGO). Their study indicated that this biosensor exhibited excellent sensing performance (detection limit of 47×10^{-9} M, linear sensing range from 0.15×10^{-6} to 900×10^{-6} M) and remained a long-term stability (>1 month).[147] Generally, the solution pH and temperature can influence the activity of enzyme, thereby influencing the biosensor response. Therefore, an optimum operating condition for improving the detection sensitivity should be carried out beforehand. Compared with enzyme immobilized biosensor, Ag–graphene nanocomposite-based optical sensor may provide simple preparation and operating procedures and excellent stability for the detection of biomolecules. AgNPs possess a sharp light adsorption feature that arise from the surface plasmon resonance (SPR), thereby allowing the application of AgNPs in optical sensors.[148,149] In 2015, a novel Ag@GO nanocomposite-based optical sensor was developed for the detection of dopamine (DA), ascorbic acid (AA), and uric acid (UA).[150] In this study, the detection limit of DA

was superior than that of AA and UA, which was attributed to the higher binding of DA with AgNPs. Meanwhile, the nature of adsorption sites and the interaction with the functional groups of molecules were responsible for the adsorption and sensing ability of Ag@GO nanocomposites.[150] Furthermore, Ag–graphene nanocomposites were also developed as biosensors for the detection of bacterial cell. An anti-SRB antibody labeled GO sheets mediated Ag enhancement has been employed for the detection of sulfate-reducing bacteria (SRB). With an electrochemical technique, the detection of cell concentration from 1.8×10^2 to 1.8×10^8 CFU mL^{-1} was obtained.[145] To date, although the studies of Ag–graphene based nanocomposites for biological sensoring are relatively limited, the published reports may open up a significant way for the application of Ag–graphene sensors in this field.

All these reports show the great potential of Ag–graphene based nanocomposites in chemical and biological sensoring. We have tabulated the detection performance of Ag–graphene based nanocomposites as sensors toward various chemical and biological targets(**Table 2**). Through comparing the detection limit, sensitivity, and cost, a better design of nanocomposite sensor can be obtained. However, the complexity of environment makes the detection accuracy more difficult. Thus, great efforts should be paid to develop stable sensors in detection field.

In addition to the above applications of Ag–graphene nanocomposites, their electronic applications are also actively investigated.[151,152] For example, it has been reported that Ag–graphene hybrids could be used as conductive ink for writing electronics and as fiber electrodes in flexible fiber-type transistors.[153,154] Overall, there is an extensive application of Ag–graphene nanocomposites in various fields. Thus, much work should be carried out to give a comprehensive knowledge of Ag–graphene nanocomposites.

6. Challenges and Perspectives

Ag–graphene based nanocomposites are no doubt playing important roles in various fields due to their exceptional properties. Researches relating to these nanocomposites have increased sharply in a variety of disciplines. This Review states the research and application value of Ag–graphene based nanocomposites. It is the first report that fully illustrates their synthesis and applications as antimicrobial agents, catalysts, and sensors in biomedicine, environment remediation and detection, and agricultural protection, etc. However, these researches are still in an initial stage. Numerous potential challenges will hamper the development of these nanocomposites. Hence, a great deal of work needs to be carried out to reduce the technology bottleneck

Table 2. The detection performance of Ag–graphene based nanocomposites on various chemical and biological targets.

Materials	Targets	Analytical methods	Detection limit	Linear response range	Reference
Ag octahedron @GO	Crystal violet	SERS	1×10^{-9} M		[132]
	Rhodamine 6G		0.1 nm		
rGO/AgNPs	Crystal violet	SERS	0.1 nm		[28]
Ag–rGO/Si	Rhodamine B	SERS	1×10^{-9} M		[133]
	Methylene blue		1×10^{-9} M		
Ag/GNs	2,4,6-Trinitrotoluene	SERS	10^{-11} M		[136]
AgNPs/CS-G	Nitrobenzene	EM	0.60 ppm	1–110 ppm	[137]
	2,4,6-Trinitrotoluene		0.45 ppm	1–70 ppm	
	2,4-Dinitrotoluene		0.21 ppm	1–110 ppm	
RGO-AgNPs	Nitrobenzene	EM	0.261×10^{-6} M	$(0.5–900) \times 10^{-6}$ M	[35]
AgNPs-GO	Arsenic(III)	EM	0.24×10^{-9} M	$(13.33–375.19) \times 10^{-9}$ M	[139]
Ag–RGO	Nitrite	EM	<1 ppm	10–1000 nm	[30]
AgP/PEI-rGO	$NaNO_2$	EM	0.1×10^{-6} M	$(2.5–13\,800) \times 10^{-6}$ M	[140]
	N_2H_4		1.0×10^{-6} M	$(5.0–17750) \times 10^{-6}$ M	
FG-Ag	*p*-Aminothiophenol	SERS	0.02×10^{-6} M		[135]
	Melamine		0.1×10^{-6} M		
Ag/ZnO-Gr	C_2H_2	EM	1 ppm	1–1000 ppm	[144]
Chitosan/GOD/AgNPs-G	Glucose	EM	100×10^{-6} M	$(2–10) \times 10^{-3}$ M	[57]
GOD/AgNP/F-siO_2/GO	Glucose	EM	310×10^{-6} M	$(2–12) \times 10^{-3}$ M	[133]
GOD-MBA-Ag@AuNPs-GO	Glucose	SERS	0.33×10^{-3} M	$(2–6) \times 10^{-3}$ M	[145]
PDH-AgNPs/rGO	L-Phenylalanine	EM	47×10^{-9} M	$(0.15–900) \times 10^{-6}$ M	[147]
Ag@GO	Dopamine	SPR intensity	49×10^{-9} M	$(0.1–2) \times 10^{-6}$ M	[150]
	Ascorbic acid		634×10^{-9} M	$(5–30) \times 10^{-6}$ M	
	Uric acid		927×10^{-9} M	$(5–50) \times 10^{-6}$ M	

and knowledge gap for the development of Ag–graphene based nanocomposites. Herein, several important issues are highlighted to provide an outline for the future research.

1) Optimize the synthesis methods of size and shape-controllable Ag nanostructures on graphene sheets: various approaches have been applied for the synthesis of Ag–graphene based nanocomposites. The main factors influencing the size, density, and shape of Ag nanostructures have been pointed out. Furthermore, the rapid one-pot synthesis routes have been proposed.[58,59] However, how to ensure the suitable size and shape obtained in a rapid procedure is still difficult, due to the diversity of synthesis conditions. For better special applications, exploring and optimizing the synthesis methods are necessary.
2) Improve the chemical stability of synthesized nanocomposites: AgNPs are dispersed on the surface of graphene sheets in most of the fabricated nanocomposites, which increases the exposure chances in external environments and substances. Thus, understanding and improving the stability of Ag–graphene based nanocomposites in the interference conditions is important for their practical applications.
3) Seek facile approaches to separate the nanocomposites from aqueous solution after catalysis: since the excellent catalytic activity toward various pollutants, a facile solid–liquid separation is vital for the regeneration. Magnetic nanomaterials have been used in wastewater treatment due to the easy separation with magnet.[155] Moreover, 3D graphene materials have been employed as catalyst supports in environmental fields due to their excellent physicochemical properties and convenient separation.[156] The two materials provide feasible methods for enhancing their separation in waste treatment, deserving further research.
4) Develop the nonenzymatic sensors for the detection of biomolecules: the immobilization of enzyme on Ag–graphene modified electrodes is complicated and usually unstable.[57,133] Nonenzymatic sensors exhibited higher stability than enzymatic sensors.[157] Zheng et al. have reported the excellent stability and high sensitivity of AgNPs/CuO nanofibers as a nonenzymatic glucose sensor.[157] Thus, it shows great potential to develop nonenzymatic sensors for the detection of biomolecules.
5) Study the effects of Ag–graphene nanocomposites on the microbial communities: Ag–graphene nanocomposites exhibit outstanding antimicrobial properties and have been applied for damaging the harmful microbes, thus, whether the coexist beneficial microbes will be affected should be taken into account. It has been reported that graphene materials will cause the unfavorable changes of microbial communities and biological functions in environment.[158] Likewise, the study on microbial communities change with Ag–graphene based nanocomposites is essential for understanding their ecosystem effects.
6) Research the fate and transport of Ag–graphene nanocomposites in environment: studies on the fate and transport of AgNPs and graphene materials have been reported, which are important to evaluate their potential risks.[5,159,160] However, the researches on the environmental behaviors of Ag–graphene based nanocomposites are limited. Hence, it is necessary to research their colloid properties and fate in water and soil environments.

Acknowledgements

K.H., Z.Z., and A.C. contributed equally to this work. The authors would like to thank Prof. J. Lee and Dr. X. Xin for their helpful English language suggestions. This study was financially supported by the National Natural Science Foundation of China (81773333, 51521006, and 51508186), the Program for Changjiang Scholars and Innovative Research Team in University (IRT-13R17), the Hunan Provincial Natural Science Foundation of China (2016JJ3076).

Conflict of Interest

The authors declare no conflict of interest.

Keywords

antimicrobial agents, catalysts, graphene, hybridization, sensors, silver nanoparticles

Received: March 5, 2018
Revised: April 7, 2018
Published online:

[1] S. Stankovich, D. A. Dikin, G. H. Dommett, K. M. Kohlhaas, E. J. Zimney, E. A. Stach, R. D. Piner, S. T. Nguyen, R. S. Ruoff, *Nature* **2006**, *442*, 282.
[2] K. S. Novoselov, V. I. Fal'ko, L. Colombo, P. R. Gellert, M. G. Schwab, K. Kim, *Nature* **2012**, *490*, 192.
[3] L. Yang, M. Zou, S. Wu, W. Xu, H. Wu, A. Cao, *ACS Nano* **2017**, *11*, 2944.
[4] K. S. Novoselov, A. K. Geim, S. V. Morozov, D. Jiang, Y. Zhang, S. V. Dubonos, I. V. Grigorieva, A. A. Firsov, *Science* **2004**, *306*, 666.
[5] K. He, G. Chen, G. Zeng, M. Peng, Z. Huang, J. Shi, T. Huang, *Nanoscale* **2017**, *9*, 5370.
[6] D. R. Dreyer, S. Park, C. W. Bielawski, R. S. Ruoff, *Chem. Soc. Rev.* **2010**, *39*, 228.
[7] Y. Zhu, S. Murali, W. Cai, X. Li, J. W. Suk, J. R. Potts, R. S. Ruoff, *Adv. Mater.* **2010**, *22*, 3906.
[8] H. Wang, X. Yuan, Y. Wu, H. Huang, X. Peng, G. Zeng, H. Zhong, J. Liang, M. Ren, *Adv. Colloid Interface Sci.* **2013**, *195–196*, 19.
[9] Y. Wang, Z. Shi, Y. Huang, Y. Ma, C. Wang, M. Chen, Y. Chen, *J. Phys. Chem. C* **2009**, *113*, 13103.
[10] X. Miao, S. Tongay, M. K. Petterson, K. Berke, A. G. Rinzler, B. R. Appleton, A. F. Hebard, *Nano Lett.* **2012**, *12*, 2745.
[11] P. T. Yin, T. H. Kim, J. W. Choi, K. B. Lee, *Phys. Chem. Chem. Phys.* **2013**, *15*, 12785.
[12] H. Sun, S. Liu, G. Zhou, H. M. Ang, M. O. Tade, S. Wang, *ACS Applied Mater. Interfaces* **2012**, *4*, 5466.
[13] S. Agnoli, M. Favaro, *J. Mater. Chem. A* **2016**, *4*, 5002.
[14] C. Xu, X. Wang, J. Zhu, *J. Phys. Chem. C* **2008**, *112*, 19841.
[15] J. Zhang, Z. Xiong, X. S. Zhao, *J. Mater. Chem.* **2011**, *21*, 3634.
[16] J. Kang, Y. Jang, Y. Kim, S. H. Cho, J. Suhr, B. H. Hong, J. B. Choi, D. Byun, *Nanoscale* **2015**, *7*, 6567.
[17] B. Li, H. Cao, *J. Mater. Chem.* **2011**, *21*, 3346.
[18] L. Hu, J. Wan, G. Zeng, A. Chen, G. Chen, Z. Huang, K. He, M. Cheng, C. Zhou, W. Xiong, *Environ. Sci.: Nano* **2017**, *4*, 2018.
[19] N. A. Luechinger, E. K. Athanassiou, W. J. Stark, *Nanotechnology* **2008**, *19*, 445201.
[20] Z. Zhang, F. Xu, W. Yang, M. Guo, X. Wang, B. Zhang, J. Tang, *Chem. Commun.* **2011**, *47*, 6440.

[21] Z. Huang, G. Chen, G. Zeng, Z. Guo, K. He, L. Hu, J. Wu, L. Zhang, Y. Zhu, Z. Song, *J. Hazard. Mater.* **2017**, *321*, 37.
[22] L. Wei, J. Lu, H. Xu, A. Patel, Z. S. Chen, G. Chen, *Drug Discovery Today* **2015**, *20*, 595.
[23] H. D. Beyene, A. A. Werkneh, H. K. Bezabh, T. G. Ambaye, *Sustainable Mater. Technol.* **2017**, *13*, 18.
[24] K. G. Stamplecoskie, J. C. Scaiano, *J. Am. Chem. Soc.* **2010**, *132*, 1825.
[25] K. He, G. Chen, G. Zeng, Z. Huang, Z. Guo, T. Huang, M. Peng, J. Shi, L. Hu, *Appl. Microbiol. Biotechnol.* **2017**, *101*, 1.
[26] Z. Guo, G. Chen, G. Zeng, J. Liang, B. Huang, Z. Xiao, F. Yi, Z. Huang, K. He, *Environ. Sci.: Nano* **2016**, *3*, 1027.
[27] W. Gao, C. Ran, M. Wang, X. Yao, D. He, J. Bai, *J. Nanopart. Res.* **2013**, *15*, 1727.
[28] Q. Huang, J. Wang, W. Wei, Q. Yan, C. Wu, X. Zhu, *J. Hazard. Mater.* **2015**, *283*, 123.
[29] S. Singh, R. K. Gundampati, K. Mitra, K. Ramesh, M. V. Jagannadham, N. Misra, B. Ray, *RSC Adv.* **2015**, *5*, 81994.
[30] A. Shaikh, S. Parida, S. Böhm, *RSC Adv.* **2016**, *6*, 100383.
[31] S. V. Kumar, N. M. Huang, H. N. Lim, A. R. Marlinda, I. Harrison, C. H. Chia, *Chem. Eng. J.* **2013**, *219*, 217.
[32] J. Li, C. Y. Liu, *Eur. J. Inorg. Chem.* **2010**, *2010*, 1244.
[33] S. Y. Lee, M. H. Chong, K. Y. Rhee, S. J. Park, *Curr. Appl. Phys.* **2014**, *14*, 1212.
[34] H. Liu, L. Zhong, K. Yun, M. Samal, *Biotechnol. Bioprocess Eng.* **2016**, *21*, 1.
[35] C. Karuppiah, K. Muthupandi, S. M. Chen, M A. Ali, S. Palanisamy, A. Rajan, P. Prakash, F. M. A. Al-Hemaid, B. S. Lou, *RSC Adv.* **2015**, *5*, 31139.
[36] X. Wang, P. Huang, L. Feng, M. He, S. Guo, G. Shen, D. Cui, *RSC Adv.* **2012**, *2*, 3816.
[37] R. Muszynski, A. Brian Seger, P. V. Kamat, *J. Phys. Chem. C* **2008**, *112*, 5263.
[38] X. Wang, C. Zhu, Z. Huang, X. Hu, X. Zhu, *RSC Adv.* **2016**, *6*, 91579.
[39] M. Nasrollahzadeh, M. Atarod, B. Jaleh, M. Gandomirouzbahani, *Ceram. Int.* **2016**, *42*, 8587.
[40] X. Qin, Y. Luo, W. Lu, G. Chang, A. M. Asiri, A. O. Al-Youbi, X. Sun, *Electrochim. Acta* **2012**, *79*, 46.
[41] J. Shen, M. Shi, N. Li, B. Yan, H. Ma, Y. Hu, M. Ye, *Nano Res.* **2010**, *3*, 339.
[42] Y. Wei, X. Zuo, X. Li, S. Song, L. Chen, J. Shen, Y. Meng, Y. Zhao, S. Fang, *Mater. Res. Bull.* **2014**, *53*, 145.
[43] W. Lu, G. Chang, Y. Luo, L. Fang, X. Sun, *J. Mater. Sci.* **2011**, *46*, 5260.
[44] A. F. de Faria, D. S. Martinez, S. M. Meira, A. C. de Moraes, A. Brandelli, A. G. Filho, O. L. Alves, *Colloids Surf., B* **2014**, *113*, 115.
[45] G. Ding, S. Xie, Y. Liu, L. Wang, F. Xu, *Appl. Surf. Sci.* **2015**, *345*, 310.
[46] B. P. Acar, *Ultrason. Sonochem.* **2017**, *35*, 397.
[47] J. Shen, M. Shi, B. Yan, H. Ma, N. Li, M. Ye, *J. Mater. Chem.* **2011**, *21*, 7795.
[48] Z. Zhang, J. Zhang, B. Zhang, J. Tang, *Nanoscale* **2013**, *5*, 118.
[49] R. Pasricha, S. Gupta, A. K. Srivastava, *Small* **2009**, *5*, 2253.
[50] J. Tian, S. Liu, Y. Zhang, H. Li, L. Wang, Y. Luo, A. M. Asiri, A. O. Al-Youbi, X. Sun, *Inorg. Chem.* **2012**, *51*, 4742.
[51] J. Li, D. Kuang, Y. Feng, F. Zhang, Z. Xu, M. Liu, D. Wang, *Biosens. Bioelectron.* **2013**, *42*, 198.
[52] W. Yuan, Y. Gu, L. Li, *Appl. Surf. Sci.* **2012**, *261*, 753.
[53] Z. Yang, C. Qi, X. Zheng, J. Zheng, *New J. Chem.* **2015**, *39*, 9358.
[54] K. S. Hui, K. N. Hui, D. A. Dinh, C. H. Tsang, Y. R. Cho, W. Zhou, X. Hong, H. H. Chun, *Acta Mater.* **2014**, *64*, 326.
[55] M. S. Yee, P. S. Khiew, W. S. Chiu, Y. F. Tan, Y. Y. Kok, C. O. Leong, *Colloids Surf., B* **2016**, *148*, 392.
[56] X. Z. Tang, Z. Cao, H. B. Zhang, J. Liu, Z. Z. Yu, *Chem. Commun.* **2011**, *47*, 3084.
[57] Y. Zhang, S. Liu, L. Wang, X. Qin, J. Tian, W. Lu, G. Chang, X. Sun, *RSC Adv.* **2012**, *2*, 538.
[58] T. Long, L. Hu, H. Dai, Y. Tang, *Appl. Phys. A* **2014**, *116*, 25.
[59] S. Liu, J. Tian, W. Lei, X. Sun, *J. Nanopart. Res.* **2011**, *13*, 4539.
[60] J. Chen, X. Zheng, H. Wang, W. Zheng, *Thin Solid Films* **2011**, *520*, 179.
[61] Y. Ji, Y. Zhang, Z. Wang, T. Zhang, *Mater. Res. Bull.* **2015**, *72*, 184.
[62] M. E. Khan, M. M. Khan, M. H. Cho, *New J. Chem.* **2015**, *39*, 8121.
[63] T. V. M. Sreekanth, M. Pandurangan, M. J. Jung, Y. R. Lee, I. Y. Eom, *Res. Chem. Intermed.* **2016**, *42*, 5665.
[64] T. V. M. Sreekanth, M. J. Jung, I. Y. Eom, *Appl. Surf. Sci.* **2016**, *361*, 102.
[65] T. Jiang, X. Wang, S. Tang, J. Zhou, C. Gu, J. Tang, *Sci. Rep.* **2017**, *7*, 9795.
[66] S. Chen, X. Li, Y. Zhao, L. Chang, J. Qi, *Carbon* **2015**, *81*, 767.
[67] J. C. Reed, H. Zhu, A. Y. Zhu, C. Li, E. Cubukcu, *Nano Lett.* **2012**, *12*, 4090.
[68] A. Zeynep, P. Jack, T. Katy-Anne, I. E. Tothill, *Biosens. Bioelectron.* **2015**, *74*, 996.
[69] S. Kaviya, J. Santhanalakshmi, B. Viswanathan, J. Muthumary, K. Srinivasan, *Spectrochim. Acta, Part A* **2011**, *79*, 594.
[70] A. Nanda, M. Saravanan, *Nanomedicine* **2009**, *5*, 452.
[71] R. Bryaskova, D. Pencheva, S. Nikolov, T. Kantardjiev, *J. Chem. Biol.* **2011**, *4*, 185.
[72] K. Krishnamoorthy, M. Veerapandian, L. H. Zhang, K. Yun, S. J. Kim, *J. Phys. Chem. C* **2012**, *116*, 17280.
[73] S. Liu, T. H. Zeng, M. Hofmann, E. Burcombe, J. Wei, R. Jiang, J. Kong, Y. Chen, *ACS Nano* **2011**, *5*, 6971.
[74] J. Chen, H. Peng, X. Wang, F. Shao, Z. Yuan, H. Han, *Nanoscale* **2014**, *6*, 1879.
[75] R. Geetha Bai, K. Muthoosamy, F. N. Shipton, A. Pandikumar, P. Rameshkumar, N. M. Huang, S. Manickam, *RSC Adv.* **2016**, *6*, 36576.
[76] A. C. de Moraes, B. A. Lima, A. F. de Faria, M. Brocchi, O. L. Alves, *Int. J. Nanomed.* **2015**, *10*, 6847.
[77] S. Barua, S. Thakur, L. Aidew, A. K. Buragohain, P. Chattopadhyay, N. Karak, *RSC Adv.* **2014**, *4*, 9777.
[78] J. Ma, J. Zhang, Z. Xiong, Y. Yong, X. S. Zhao, *J. Mater. Chem.* **2011**, *21*, 3350.
[79] B. Jiang, C. Tian, G. Song, W. Chang, G. Wang, Q. Wu, H. Fu, *J. Mater. Sci.* **2013**, *48*, 1980.
[80] T. He, H. Liu, Y. Zhou, J. Yang, X. Cheng, H. Shi, *BioMetals* **2014**, *27*, 673.
[81] B. Song, C. Zhang, G. Zeng, J. Gong, Y. Chang, Y. Jiang, *Arch. Biochem. Biophys.* **2016**, *604*, 167.
[82] W. Shao, X. Liu, H. Min, G. Dong, Q. Feng, S. Zuo, *ACS Appl. Mater. Interfaces* **2015**, *7*, 6966.
[83] M. R. Das, R. K. Sarma, R. Saikia, V. S. Kale, M. V. Shelke, P. Sengupta, *Colloids Surf., B* **2011**, *83*, 16.
[84] J. S. Kim, E. Kuk, K. N. Yu, J. H. Kim, S. J. Park, H. J. Lee, S. H. Kim, Y. K. Park, Y. H. Park, C. Y. Hwang, *Nanomedicine* **2007**, *3*, 95.
[85] Q. Bao, D. Zhang, P. Qi, *J. Colloid Interface Sci.* **2011**, *360*, 463.
[86] J. Tang, Q. Chen, L. Xu, S. Zhang, L. Feng, L. Cheng, H. Xu, Z. Liu, R. Peng, *ACS Appl. Mater. Interfaces* **2013**, *5*, 3867.
[87] B. Pant, P. Pokharel, A. P. Tiwari, P. S. Saud, M. Park, Z. K. Ghouri, S. Choi, S. J. Park, H.-Y. Kim, *Ceram. Int.* **2015**, *41*, 5656.
[88] E. I. Rabea, M. E. Badawy, C. V. Stevens, G. Smagghe, W. Steurbaut, *Biomacromolecules* **2003**, *4*, 1457.
[89] D. Wei, W. Sun, W. Qian, Y. Ye, X. Ma, *Carbohydr. Res.* **2009**, *344*, 2375.
[90] B. Marta, M. Potara, M. Iliut, E. Jakab, T. Radu, F. Imre-Lucaci, G. Katona, O. Popescu, S. Astilean, *Colloids Surf., A* **2015**, *487*, 113.

[91] L. V. Jankauskait, L. A. Vitkauskien, A. Lazauskas, J. Baltrusaitis, I. ProsyLevas, M. AndruleviLius, *Int. J. Pharm.* **2016**, *511*, 90.
[92] A. Naskar, S. Bera, R. Bhattacharya, P. Saha, S. S. Roy, T. Sen, S. Jana, *RSC Adv.* **2016**, *6*, 88751.
[93] E. Roy, S. Patra, A. Tiwari, R. Madhuri, P. K. Sharma, *Biosens. Bioelectron.* **2017**, *89*, 620.
[94] M. Auffan, W. Achouak, J. Rose, M. A. Roncato, C. Chanéac, D. T. Waite, A. Masion, J. C. Woicik, M. R. Wiesner, J. Y. Bottero, *Environ. Sci. Technol.* **2008**, *42*, 6730.
[95] H. Z. Zhang, C. Zhang, G. M. Zeng, J. L. Gong, X. M. Ou, S. Y. Huan, *J. Colloid Interface Sci.* **2016**, *471*, 94.
[96] J. Mansouri, S. Harrisson, V. Chen, *J. Mater. Chem.* **2010**, *20*, 4567.
[97] J. Li, X. Liu, J. Lu, Y. Wang, G. Li, F. Zhao, *J. Colloid Interface Sci.* **2016**, *484*, 107.
[98] X. F. Sun, J. Qin, P. F. Xia, B. B. Guo, C. M. Yang, C. Song, S. G. Wang, *Chem. Eng. J.* **2015**, *281*, 53.
[99] A. F. Faria, C. Liu, M. Xie, F. Perreault, D. N. Long, J. Ma, M. Elimelech, *J. Membr. Sci.* **2017**, *525*, 146.
[100] A. Soroush, W. Ma, Y. Silvino, M. S. Rahaman, *Environ. Sci.: Nano* **2015**, *2*, 395.
[101] I. Ocsoy, M. L. Paret, M. A. Ocsoy, S. Kunwar, T. Chen, M. You, W. Tan, *ACS Nano* **2013**, *7*, 8972.
[102] J. Chen, L. Sun, Y. Cheng, Z. Lu, K. Shao, T. Li, C. Hu, H. Han, *ACS Appl. Mater. Interfaces* **2016**, *8*, 24057.
[103] D. Cantillo, M. M. Moghaddam, C. O. Kappe, *J. Org. Chem.* **2013**, *78*, 4530.
[104] O. A. O'Connor, L. Young, *Environ. Toxicol. Chem.* **1989**, *8*, 853.
[105] J. D. Kim, H. C. Choi, *Bull. Korean Chem. Soc.* **2015**, *36*, 2404.
[106] Y. Li, Y. Cao, J. Xie, D. Jia, H. Qin, Z. Liang, *Catal. Commun.* **2015**, *58*, 21.
[107] N. Meng, S. Zhang, Y. Zhou, W. Nie, P. Chen, *RSC Adv.* **2015**, *5*, 70968.
[108] B. Paul, D. D. Purkayastha, S. S. Dhar, S. Das, S. Haldar, *J. Alloys Compd.* **2016**, *681*, 316.
[109] H. Tong, S. Ouyang, Y. Bi, N. Umezawa, M. Oshikiri, J. Ye, *Adv. Mater.* **2012**, *24*, 229.
[110] C. Zeng, M. Guo, B. Tian, J. Zhang, *Chem. Phys. Lett.* **2013**, *575*, 81.
[111] J. Low, J. Yu, Q. Li, B. Cheng, *Phys. Chem. Chem. Phys.* **2014**, *16*, 1111.
[112] C. J. Miller, H. Yu, T. D. Waite, *Colloids Surf. A* **2013**, *435*, 147.
[113] X. H. Meng, X. Shao, H. Y. Li, F. Z. Liu, X. P. Pu, W. Z. Li, C. H. Su, *Mater. Res. Bull.* **2013**, *48*, 1453.
[114] K. Hareesh, R. P. Joshi, S. S. Dahiwale, V. N. Bhoraskar, S. D. Dhole, *Vacuum* **2016**, *124*, 40.
[115] M. Faraji, N. Mohaghegh, *Surf. Coat. Technol.* **2016**, *288*, 144.
[116] J. Lu, H. Wang, S. Dong, F. Wang, Y. Dong, *J. Alloys Compd.* **2014**, *617*, 869.
[117] J. Hu, Y. Liu, J. Men, L. Zhang, H. Huang, *Solid State Sci.* **2016**, *61*, 239.
[118] Y. Wen, H. Ding, Y. Shan, *Nanoscale* **2011**, *3*, 4411.
[119] W. Zhao, Z. Zhang, J. Zhang, H. Wu, L. Xi, C. Ruan, *Mater. Lett.* **2016**, *171*, 182.
[120] L. Xu, Y. Wei, W. Guo, Y. Guo, Y. Guo, *Appl. Surf. Sci.* **2015**, *332*, 682.
[121] E. H. Umukoro, M. G. Peleyeju, J. C. Ngila, O. A. Arotiba, *RSC Adv.* **2016**, *6*, 52868.
[122] S. K. Bhunia, N. R. Jana, *ACS Appl. Mater. Interfaces* **2014**, *6*, 20085.
[123] L. Liu, H. Bai, J. Liu, D. D. Sun, *J. Hazard. Mater.* **2013**, *261*, 214.
[124] C. Cui, Y. Wang, D. Liang, W. Cui, H. Hu, B. Lu, S. Xu, X. Li, C. Wang, Y. Yang, *Appl. Catal., B* **2014**, *158–159*, 150.
[125] Y. Yu, Y. Liu, X. Wu, Z. Weng, Y. Hou, L. Wu, *Sep. Purif. Technol.* **2015**, *142*, 1.
[126] J. Hu, J. Men, Y. Liu, H. Huang, T. Jiao, *RSC Adv.* **2015**, *5*, 54028.
[127] L. Qin, G. Zeng, C. Lai, D. Huang, C. Zhang, P. Xu, T. Hu, X. Liu, M. Cheng, Y. Liu, *Sens. Actuators, B* **2017**, *243*, 946.
[128] L. Tang, X. Lei, G. Zeng, Y. Liu, Y. Peng, M. Wu, Y. Zhang, C. Liu, Z. Li, G. Shen, *Spectrochim. Acta, Part A* **2012**, *99*, 390.
[129] C. Zhang, C. Lai, G. Zeng, D. Huang, L. Tang, C. Yang, Y. Zhou, L. Qin, M. Cheng, *Biosens. Bioelectron.* **2016**, *81*, 61.
[130] M. Z. Si, Y. P. Kang, R. M. Liu, *Appl. Surf. Sci.* **2012**, *258*, 5533.
[131] C. Zhu, G. Meng, Q. Huang, Z. Huang, *J. Hazard. Mater.* **2003**, *99*, 389.
[132] W. Fan, Y. H. Lee, S. Pedireddy, Q. Zhang, T. Liu, X. Y. Ling, *Nanoscale* **2014**, *6*, 4843.
[133] G. Lu, H. Li, C. Liusman, Z. Yin, S. Wu, H. Zhang, *Chem. Sci.* **2011**, *2*, 1817.
[134] M. Rycenga, C. M. Cobley, J. Zeng, W. Li, C. H. Moran, Q. Zhang, D. Qin, Y. Xia, *Chem. Rev.* **2011**, *111*, 3669.
[135] S. V. Kumar, N. M. Huang, H. N. Lim, M. Zainy, I. Harrison, C. H. Chia, *Sens. Actuators, B* **2013**, *181*, 885.
[136] M. Liu, W. Chen, *Biosens. Bioelectron.* **2013**, *46*, 68.
[137] X. Lu, H. Qi, X. Zhang, Z. Xue, J. Jin, X. Zhou, X. Liu, *Chem. Commun.* **2011**, *47*, 12494.
[138] W. Liu, C. Li, Y. Gu, L. Tang, Z. Zhang, M. Yang, *Electroanalysis* **2013**, 2367.
[139] R. A. Dar, N. G. Khare, D. P. Cole, S. P. Karna, A. K. Srivastava, *RSC Adv.* **2014**, *4*, 14432.
[140] J. Wang, G. Zhang, W. Sun, J. Sun, L. Luo, Z. Chang, X. Sun, *Chem. – Eur. J.* **2016**, *22*, 10923.
[141] A. S. M. Iftekhar Uddin, K. W. Lee, G. S. Chung, *Sens. Actuators, B* **2015**, *216*, 33.
[142] Q. T. Tran, H. T. M. Hoa, D. H. Yoo, T. V. Cuong, S. H. Hur, J. S. Chung, E. J. Kim, P. A. Kohl, *Sens. Actuators, B* **2014**, *194*, 45.
[143] T. Kavinkumar, S. Manivannan, *Ceram. Int.* **2016**, *42*, 1769.
[144] A. S. M. Iftekhar Uddin, D. T. Phan, G. S. Chung, *Sens. Actuators, B* **2015**, *207*, 362.
[145] Y. Wan, Y. Wang, J. Wu, D. Zhang, *Anal. Chem.* **2011**, *83*, 648.
[146] V. K. Gupta, N. Atar, M. L. Yola, M. Eryilmaz, H. Torul, U. Tamer, I. H. Boyaci, Z. Ustundag, *J. Colloid Interface Sci.* **2013**, *406*, 231.
[147] E. Omidinia, S. M. Naghib, A. Boughdachi, P. Khoshkenar, D. K. Mills, *Int. J. Electrochem. Sc.* **2015**, *10*, 6833.
[148] G. Maduraiveeran, R. Ramaraj, *J. Nanopart. Res.* **2011**, *13*, 4267.
[149] P. Rameshkumar, S. Manivannan, R. Ramaraj, *J. Nanopart. Res.* **2013**, *15*, 1639.
[150] K. Zangeneh Kamali, A. Pandikumar, G. Sivaraman, H. N. Lim, S. P. Wren, T. Sun, N. M. Huang, *RSC Adv.* **2015**, *5*, 17809.
[151] J. Liang, L. Li, K. Tong, Z. Ren, W. Hu, X. Niu, Y. Chen, Q. Pei, *ACS Nano* **2014**, *8*, 1590.
[152] C. Wu, L. Fang, X. Huang, P. Jiang, *ACS Appl. Mater. Interfaces* **2014**, *6*, 21026.
[153] L. Y. Xu, G. Y. Yang, H. Y. Jing, J. Wei, Y. D. Han, *Nanotechnology* **2014**, *25*, 055201.
[154] S. S. Yoon, K. E. Lee, H. J. Cha, D. G. Seong, M. K. Um, J. H. Byun, Y. Oh, J. H. Oh, W. Lee, J. U. Lee, *Sci. Rep.* **2015**, *5*, 16366.
[155] P. Xu, G. M. Zeng, D. L. Huang, C. L. Feng, S. Hu, M. H. Zhao, C. Lai, Z. Wei, C. Huang, G. X. Xie, *Sci. Total Environ.* **2012**, *424*, 1.
[156] Y. Shen, Q. Fang, B. Chen, *Environ. Sci. Technol.* **2015**, *49*, 67.
[157] B. Zheng, G. Liu, A. Yao, Y. Xiao, J. Du, Y. Guo, D. Xiao, Q. Hu, M. M. F. Choi, *Sens. Actuators, B* **2014**, *195*, 431.
[158] F. Ahmed, D. F. Rodrigues, *J. Hazard. Mater.* **2013**, *256-257*, 33.
[159] L. J. Ellis, E. Valsami-Jones, J. R. Lead, M. Baalousha, *Sci. Total Environ.* **2016**, *568*, 95.
[160] W. Zhou, Y. L. Liu, A. M. Stallworth, C. Ye, J. J. Lenhart, *Environ. Sci. Technol.* **2016**, *50*, 12214.